Journal of Electrical and Electronics Engineering (IOSR-JEEE)
e-ISSN: 2278-1676, p-ISSN: 2320-3331, Volume 21, Issue 1 Ser. 1 (Jan. – Feb. 2026), PP 22-28
www.iosrjournals.org

Structural Characterization Of Nanocrystalline CdS: Mn^{+2} Ions Synthesized Thin Films For Device And Applications

M. Malemnganbi, K. Zeetibala, M. Rajesh Singh And K. Kunjabali Singh
Departrment Of Physical Science
Khongnangthaba University, Khurai-795010, Manipur.

Abstract:
Thin films of CdS: Mn^{+2} ions were synthesized in the ionic concentrations in the range 1at. %≤ m ≤9at% onto silicon wafer substrates by SILAR technique. FESEM and XRD techniques were used to study the surface morphology, crystal structures, residual stress, strains and dislocation density in the films respectively. The grain sizes in the host samples were evaluated and observed lying between 13nm-35nm in the desired nanometer range. The size of the doped CdS nanoparticles were observed to decrease with increase of Mn^{+2}-ion concentrations, as observed in the FESEM morphology. The as deposited CdS: Mn^{+2}films showed bcc as crystal structures which is cubic at 5at. % Mn^{+2} doped ions and fcc cubic at CdS: 9at% Mn^{+2} ions. The observed lattice parameters were found increasing with decreasing of the X-rays intensity and attain maximum reflection planes (221) at 1at. %, (321) and (221) at.3at % and, 5at%, (320) at 7at%, and (211) at 9at%. The observed a and d-values were found decreased in parallel with intensity of X-rays. It was observed that the as deposited CdS: Mn^{+2} nanocrystalline thin films showed higher residual stress at 100% X-rays peak intensity than that of average values of the films at all levels of peak intensity.

Keywords*: Cadmium Sulphide, doping, SILAR, XRD, FESEM, crystal structure*

Date of Submission: 28-01-2026 Date of Acceptance: 08-02-2026

I. Introduction

Bulk Cadmium Sulphide (CdS) semiconductor possesses a direct band gap of 2.4eV and is one of the prominent binary II-VI compound semiconductors. Thin films of this compound find technological applications of n-type thin films heterojunction solar cells [1-3], visible radiation sensors [4-7], quantum dot single electron n transistors and UV-light emitting diodes [8-11]. Therefore, a large number of scientists and research scholars all over the world have taken considerable attention in synthesis and characterization of CdS thin films doped and undoped by several deposition techniques like thermal evaporation [12,13], r.f. sputtering [14], chemical bath deposition [15,16], sol. Gel spin coating [17], SILAR(**Successive Ionic Layer Adsorption and Reaction**) technique [18-20], hydrothermal process [21]. However, the basic criteria of semiconducting thin film deposition is to obtain uniform and stoichiometric thin film layer over large surface area with less economic and time consumption. Considering this-aspects, SILAR technique was used to deposit CdS thin films doped with manganese ions and characterized.

II. Materials And Method

We prepared 0.2M $CdCl_2$ H_2O solution by dissolving 4.03gms of $CdCl_2$ H_2O in 100ml of DI water and stirred for 30mins at room temperature.

Preparation of 2 wt.% PVA solution:

We dissolved 2gms of PVA (Polyvinyl Alcohol) in 100ml DI water and stirred at 70^0C for 30mins till PVA dissolves. Then, 50ml of $CdCl_2$ solution was mixed with 50ml PVA solution in 250ml beaker.

Preparation of $MnCl_2$ doping solution at 1at.% of Mn^{+2} ions:

We dissolved 0.63gm of $MnCl_2$ (estimated by calculation) in 50ml DI water and stirred for 5mins at room temperature. The two precursor solutions were mixed and stirred constantly for 5mins at room temperature. Properly cleaned glass substrates/Silicon wafer (4nos.) were clamped vertically in the solution for 24hrs.

We prepared 0.2M of thiourea, $CS(NH_2)_2$ by dissolving 1.52gm in 100ml DI water and stirred for 5mins at room temperature. Then, 10ml of trisodium citrate was added in the precursor solution. A few drops of ammonia solution was dropped –wise in it to adjust the pH –value at 8 – 10 and stirred constantly for

5mins at room temperature. The Cd^{+2} pre-deposited substrates were then dipped vertically into the solution for 24hrs when the Cd^{+2} –ions reacted with the S^{-2} –ions to produce CdS films doped at 1 at. % Mn^{+2} ions.

III. Results And Discussion

Surface morphology:

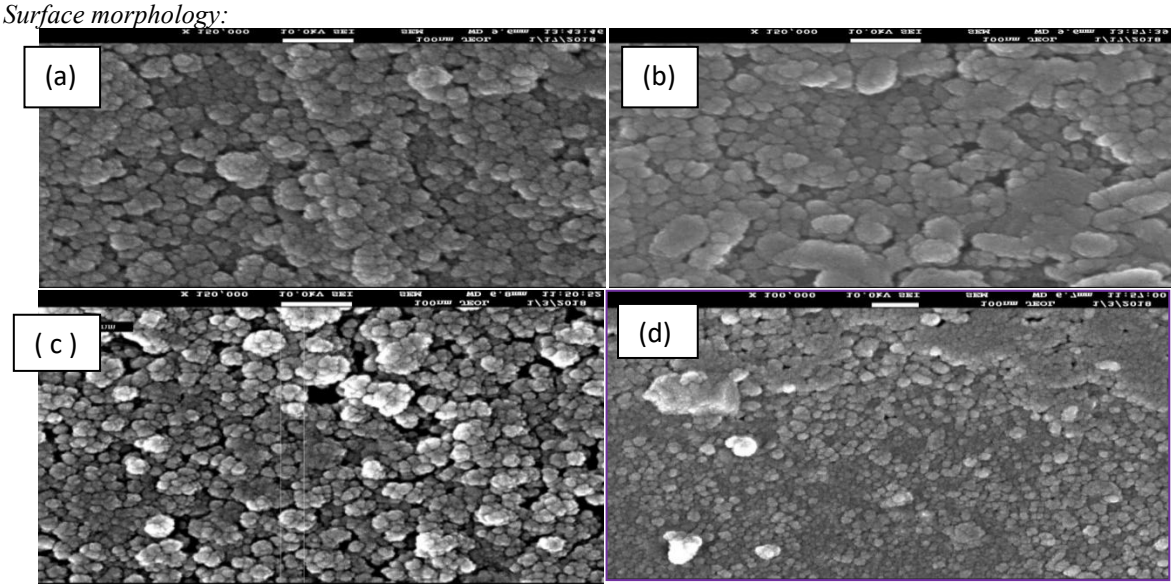

Fig.1. FESEM Surface Morphology Of Synthesized CdS: Mn^{+2} Ions
(A) 3at. % (B) 5at. % (C) 7at. % (D) 9 At. %

The as synthesized CdS doped thin films were annealed in electronic oven at 350^0C for 24hrs, cleaned in running DI water and dried for removal of course unwanted grains. The host samples were then taken FESEM **(Field Emission Scanning Electron Microscope)** and XRDs. The study of the surface morphology of the host films as shown in FESEM images (Fig. 1.) that the grown films at all doping ranges were found to be with uniform distribution of CdS grains without cracks or holes . However, the grain sizes of the CdS films were found to decrease nonlinearly with increase of Mn^{+2} –ions dopings. The grain sizes were determined in co-relation with Mn^{+2} – ions concentrations.

XRD-Spectral Analysis

The analysis of the XRD spectra of the films (Figs. 2-5) show that the number of peaks and peak intensity increase linearly with increase of Mn^{+2}-ions concentration in the CdS thin films. Also the X-ray diffraction planes from the crystals were found (100) at 1at.%, (100), (200), (211) at 5at.%(100), (200) and (211) at. 7at.% of Mn^{+2}-ions concentrations and revealed that the as grown films improved in crystallinity with the implanted Mn^{+2} – ions.

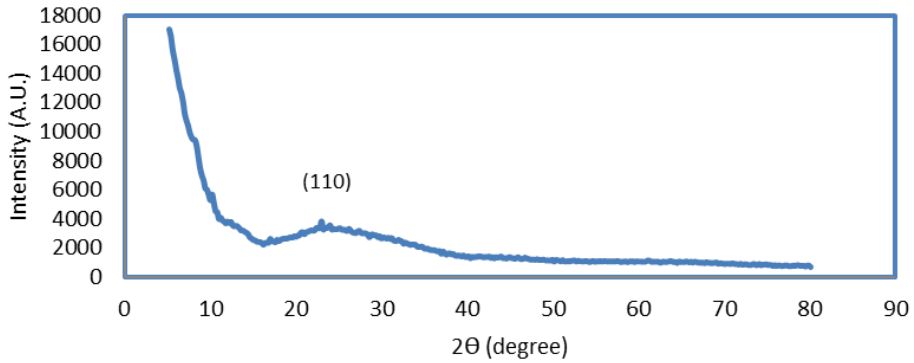

Fig. 2. XRD pattern of CdS thin films grown at 1 at.%. Mn^{+2}

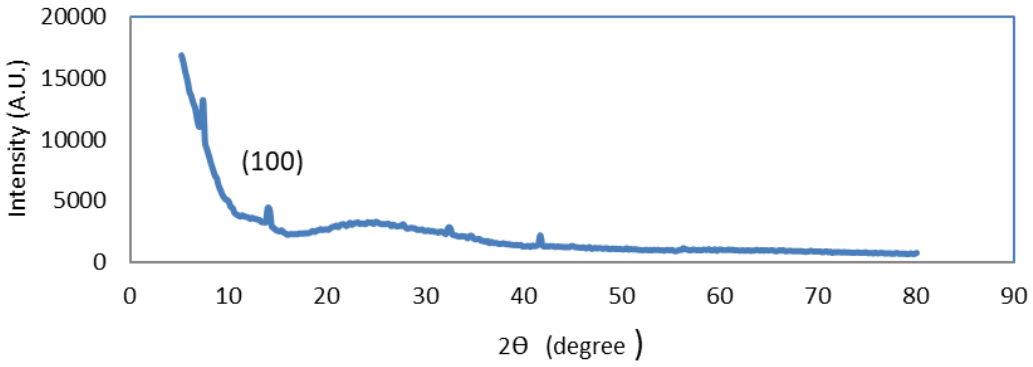

Figure 3. XRD pattern of 3 at.% Mn^{+2} iond doped CdS films.

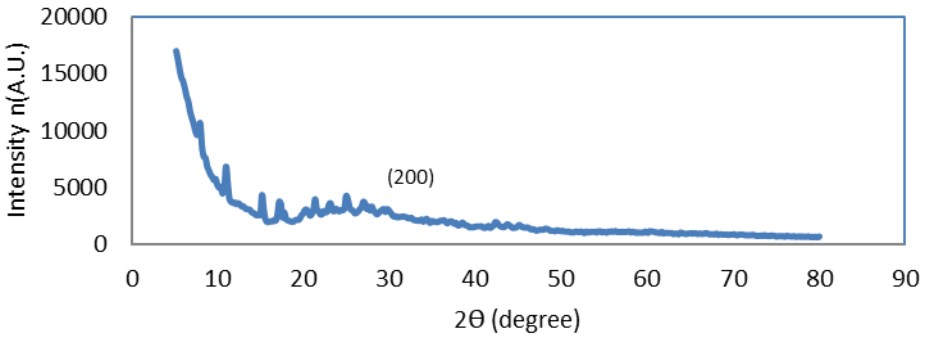

Figure 4.. XRD pattern of5 at.% Mn^{+2} doped CdS thin films.

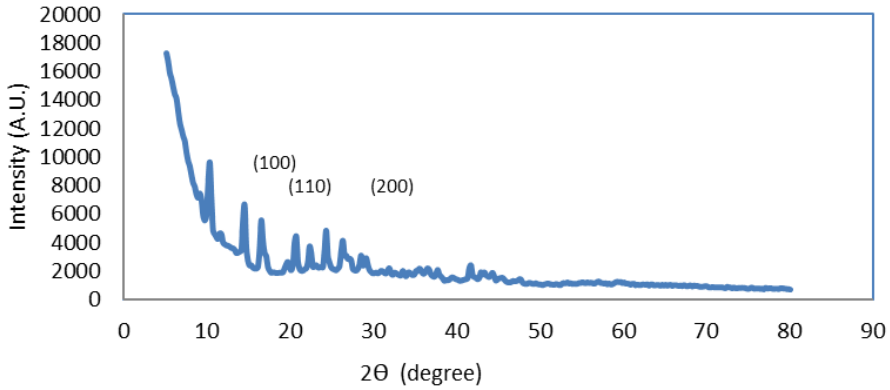

Figure 5. XRD pattern of CdS thin films doped Mn^{+2}. at 7 at.% Mn^{+2}.

Table-1. Observed lattice parameters in the crystal.

Mn^{+2}-doze	*Rel. Int. of X-rays*	*2Θ (deg)*	*(hkl)*	*JCDPS-value (Å)*	*a_{cal}-value (Å)*	*JCDPS-d-value (Å)*	*d_{cal}-value (Å)*
1 at.%	100.00	11.63	100		7.599		7.599
	76.47	19.82	100		4.470		4.470
	89.34	23.16	110		5.425		3.836
	6.37	49.13	221		5.557	2.06	1.852
3 at.%	100.00	10.05					
	25.69	11.60	100		7.617		7.617
	25.34	20.08	110		10.776		4.427
	64.79	34.31	200		5.221	2.90	2.611
	2.79	65.52	321		5.324		1.412
	39.21	66.10	321	5.83	5.282		1.412

5 at.%	29.12	5.14					
	100.00	10.04					
	64.83	11.63	100		7.803		7.603
	3.37	15.13	100		5.851		7.603
	25.25	20.01	100		4.432		4.432
	18.65	23.43	110		5.363		3.792
	15.64	25.23	110		4.986		3.525
	19.34	28.04	111		5.506		3.179
	13.67	31.12	200		5.740		2.870
	12.58	43.99	211		5.036		2.056
	8.26	45.98	220		5.575		1.971
7 at.%	100.00	5.260			**1.678**		16.782
	40.78	20.026	100		4.429		4.429
	8.92	61.344	320		5.442		1.509
9 at.%	100.00	10.170			1.738		8.688
	98.69	11.658	100		7.582		7.582
	29.20	12.634	100		6.998		6.998
	44.51	20.052	100		4.423		4.423
	45.59	23.391	110		5.372		3.798
	52.60	31.110	200		5.743		2.871
	26.89	43.943	211		5.041		2.058

The analysis of the XRD spectra of the films (Figs. 2 - 5) showed that the number of peaks and peak intensity increased linearly with increase of Mn^{+2}-ions concentration in the CdS thin films.

The X-ray diffraction planes corresponding to the peak intensity in the spectra were calculated from the Bragg's relation

$$Sin^2\Theta = (\boldsymbol{\lambda}^2/4a^2) \times m \qquad (\because 2dSin\Theta = n\boldsymbol{\lambda}) \qquad (1)$$

where $m = h^2 + k^2 + l^2$ and $\boldsymbol{\lambda} = 1.54$Å for X-rays. The crystal lattice parameters **a** and ***d*** –values were determined from the relation

$$a = (\boldsymbol{\lambda}/2Sin\Theta) \times m \qquad (2)$$

and

$$d = \boldsymbol{\lambda}/2Sin\Theta \qquad (3)$$

The diffraction planes from the crystals were found (100) at 1at.%, (100), (200), (211) at 5at.%, (100), (200) and (211) at. 7at.% of Mn^{+2}-ions concentrations and clearly revealed that the as grown CdS thin films improved in crystallinity with the implanted Mn^{+2} – ions. The Crystal structure of the synthesized host films were determined by means of $\mathbf{Sin^2\Theta_1 / Sin^2\Theta_2}$ - ratio] and found cubic zinc blend structures as shown in **Table-2**. The evaluated values of crystal miller indices and lattice parameters are shown in **Table-1**.

The grain or particle diameters were calculated at 100% X-rays intensity from the Scherrer relation [22, 23]

$$D = k\boldsymbol{\lambda}/\beta_{2\Theta}\ Cos\Theta \qquad (4)$$

where the shape factor k is taken 0.94 and for X-ray, $\boldsymbol{\lambda} = 1.54$Å, $\beta_{2\Theta}$ is the full-width half maximum peak intensity . The values of grain sizes in the films have been shown in **Table-3**.

Table-2. Determination of crystal structures of the host samples.

Mn^{+2}	$h_1k_1l_1$	$h_2k_2l_2$	Θ_1 (deg)	Θ_2 (deg)	$Sin^2\Theta_1/Sin^2\Theta_2$	$h_1^2+k_1^2+l_1^2 / h_2^2+k_2^2+l_2^2$	Crys. Str.
1 at.%	100	110	9.908	11.578	0.104	0.5	bcc (cub.)
3 at.%	110	200	10.016	17.153	0.315	0.5	bcc (cub.)
5 at.%	100	110	10.005	11.716	0.715	0.5	fcc (cub.)
7 at.%	100	320	10.013	30.672	0.116	0.07	
9 at.%	100	110	10.026	11.695	0.715	0.5	fcc (cub.)

The crystal structures of the host sample materials were calculated from the relation [24]

$$Sin^2\Theta_1/Sin^2\Theta_2 = (h_1^2+k_1^2+l_1^2)/(h_2^2+k_2^2+l_2^2) \qquad (5)$$

and were found to be bcc and f.c.c. cubic zinc sulphide structures as shown in **Table-2**.

The evaluated grain sizes in the films were found to exist between 13nm to 30nm in the nanometer range. The change in grain size vs. the doping ion concentration in the synthesized CdS thin films is shown in Fig. 6.

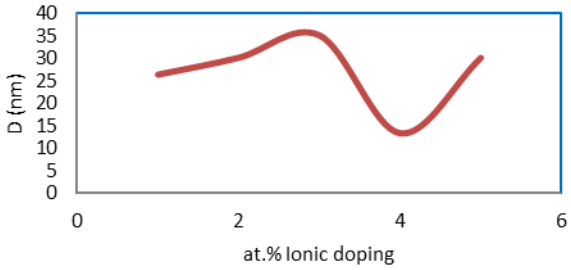

Figure 6. Grain size vs. Mn^{+2} ions in CdS thin films

Dislocation density, residual strains and stress

The intergrain crystalline states like dislocation density, residual stress and strains in the films play crucial roles in the optical, magnetic and optoelectronic properties of the films for device and applications. Such dislocation density in the host CdS films were calculated from the relation [25,26,27]

$$\delta = 1/D^2 \qquad (6)$$

in lines/m^2 where D is the particle diameter in the films. The residual strains between lattice atoms were calculated from the relation [28]

$$\varepsilon = \beta_{2\theta} \times \text{Cot}\theta/4 \qquad (7)$$

The residual stresses were calculated from the relation [29]

$$S = E/2\gamma \times (a_0 - a)/a_0 \qquad (8)$$

where a_0 = bulk value, a for the film, γ the Poisson ratio relative to CdS (= 0.38) and E Young's modulus of elasticity of the sample CdS (= 42GPa) [ ]. The evaluated residual stress and strains in the films at 100% X-rays intensity and other than 100% X-rays intensity for average have been shown in **Table- 3** and **Table – 4** respectively for comparison.

Table-3. Observed grain sizes, residual stress and strain at 100% X-ray intensity.

Sample CdS : Mn^{+2}	FWHM 2Θ (deg)	Grain Size (nm)	Dislocation density (lines/m^2) x 10^{14}	Residual strain x 10^{-2}	JCPDS a_0-value (Å)	a_{cal}-value (Å)	Residual stress (GPa)
1 at.%	0.31	26.37	14.38	50.02	5.830	7.599	2.422
3 at.%	0.28	30.14	11.01	50.02		1.759	5.572
5 at.%	0.24	35.16	8.09	50.02		1.760	5.571
7 at.%	0.63	13.18	57.57	50.02		1.678	5.683
9 at.%	0.28	30.14	11.01	50.02		1.738	5.602

The change in dislocation density vs. change in doping Mn^{+2}-ion concentrations is shown in Fig. 7 while the corresponding variation of residual strains and stress in Fig. 8 and Fig. 9 respectively.

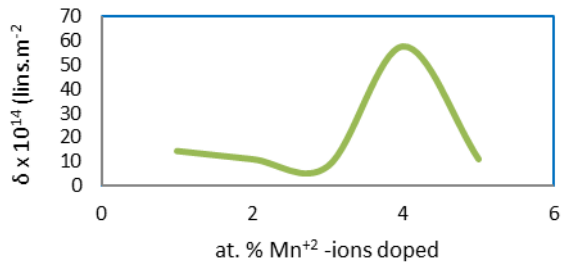

Figure 7. Dislocation density vs. Doping ions

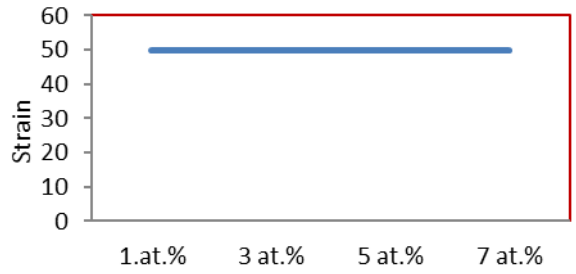

Figure 8. Residual strains vs. Doping ions

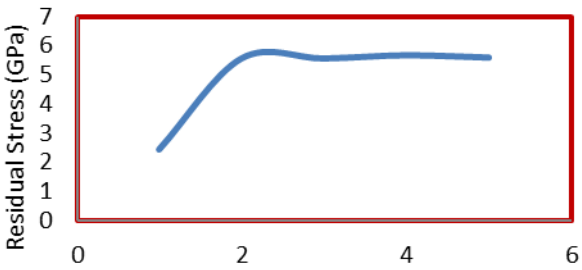

Figure 9. Residual stress vs. Doping ions .

Table-4. Average residual stress in the host samples

Mn^{+2}- ions	Rel. X-ray intensity	a_{cal}-value (Å)	Av. value of a_{cal} (Å)	JCPDS value of a_0 (Å)	Av. residual stress (GPa)
1 at.%	100.00		5.763	5.830	0.092
	76.47	4.470			
	89.34	5.425			
	6.37	5.557			
3 at.%	100.00		5.813		1.245
	25.69	7.617			
	25.34	10.776			
	64.79	5.221			
	2.79	5.324			
	39.21	5.282			
5 at.%	29.12		5.364		0.637
	100.00				
	64.83	7.803			
	3.37	5.851			
	25.25	4.432			
	18.65	5.363			
	15.64	4.986			
	19.34	5.506			
	13.67	5.740			
	12.58	5.036			
	8.26	5.575			
7 at.%	100.00		4.936		1.224
	40.78	4.429			
	8.92	5.442			
9 at.%	100.00		5.859		0.039
	98.69	7.582			
	29.20	6.998			
	44.51	4.423			
	45.59	5.372			
	52.60	5.743			
	26.89	5.041			

A comparative study of the observations showed that the as synthesized doped CdS thin films show higher stress at 100% X-rays peak intensity , however observed remarkable stress in average residual stress with increase of Mn^{+2} – ions concentrations in the CdS films (**Table**-3 & **Table**-4).These residual stress in the crystals may be explained on account of some lattice defects, non-uniform thermal expansion coefficient, mismatching materials or plastic deformation during the synthesis of the host crystal material and are expected to be controlled or minimized through controlled cooling [30].

IV. Conclusion

SILAR technique is inexpensive process for synthesis of wide range of semiconducting thin films. FESEM –surface topographic images of CdSe: Mn^{+2}-ionic concentrations were found with uniform distributions of CdS nanoparticles devoid of cracks or holes whose grain sizes were found between 13nm to 35nm as confirmed from the XRD results. The XRD spectra showed improvement of crystallization with Mn^{+2}-ionic concentrations whose crystal structures were found to be cubic bcc and fcc zinc blend structures as confirmed from $Sin^2\Theta$-ratios. The evaluated crystal lattice parameters ***a*** and ***d*** –values decreased linearly with decrease of X-rays intensity and approached to the corresponding JCPDS values.

The interstatial crystallographic structures revealed the presence of residual stress and strains. The residual stresses will have the possibility of negative impacts to the potential applications of the CdS doped thin films and need to be minimized by proper control cooling.

Acknowledgements

The authors acknowledged and thankful to CIF, Tezpur (central) University, Assam for providing FESEM images of the samples. We are also thankful and acknowledged the authorities of SAIF centre of Guwahati University, Assam for providing timely the XRD results of the samples in details.

References

[1]. K L Chopra And S R Das, Thin Film Solar Cells (New York : Plenum) (1983) 296
[2]. R H Bube Et Al, IEEE Trans Electron Devices 31 (1984)528
[3]. K C Mandal, S Basu And D N Bose, Solar Cells 18 (1986) 25
[4]. G Entinu Et Al, IEEE Trans Nuclear Sci. 28 9(1981) 558
[5]. O Yoshie, Jap, J. Appl. Phys. 15 (1976) 87
[6]. K K Nanda, S N Sarangi And S N Sahu, Curr. Sci. 72 (1997) 110
[7]. E Monroy, F Omnes And F Calle, Semicon. Sci. Technol. 18 (2003) 33
[8]. Vijay Sing, A Ranjan V, M Kaper, Bull Mater. Sci., 569 (1999) 22563
[9]. K K Nanda, S N Sarangi And S N Sahu, Nano Structural Matter, 10 (1998) 1401
[10]. D Mahanta, S K Dolui, A Choudhury, Indian J Phys. 75A (2001) 53
[11]. J Barman, K C Sarma, M Sarma And K Sarma, Indian Journal Of Pure & Applied Physics Vol. 46 May, (2008) 339-343
[12]. K Kunjabali Singh And H L Das, Indian J. Phys. 82(6) (2008) 685-693
[13]. M Melvin, David Kumar, Singanthe Devadason, Appl. Nanosci. 3 (2013) 453-459
[14]. Tra Arh Khoa Nguyen Et Al./ Nanomaterials 13 (2023) 2677
[15]. M P Deshpande, S H Chaki, N H Patel, S V Bhatt, B H Soni, J. Nano-Electron Phys. 3 No. 1 (2011) 193-202
[16]. M Dinendra Singh And K Kunjabali Singh, IOSR Journal Of Applied Physics (IOSR-JAP) Vol. 16, Issue 2 Ser. 1 (Mar-Apr. 2024) 12-16
[17]. Ksh Priyalakshmi Devi, Pranab Goswami, Harsh Choturvedi, Applied Surface Science Vol. 591 30 July (2022)153225
[18]. H M Pathan, B R Sankapal, J D Desai, C D Lokhande, Material Chemistry And Physics 78 (2002) 11-14
[19]. H Jamuna Devi, Ksh Nandini Devi, M Rashmani Devi And K Kunjabali Singh, IOSR Journal Of Applied Physics (IOSR-JAP) Vol. 16, Issue 4 Ser 1 (Jul-Aug, 2024) 01-07
[20]. K Zeetibala, M Rajesh Singh, M Malemnganbi And K Kunjabali Singh, Journal Of Electrical And Electronics Engineering (IOSR-JEEE) Vol. 20, Issue 6 Ser. 1 (Nov-Dec., 2025) 31-36
[21]. R G Setelo Et Al, Solar Energy Vol. 301, 15 November, (2025) 113942
[22]. H P Klug And L E Alexander, X-Ray Diffraction Procedures, New York, John Willey & Sons Inc., (1954) 490
[23]. K. Kunjabali Singh And H. L. Das, Microstructures, Stress, Strain And Surface Characterization Of TD Polycrystalline Cds Thin Films, Indian J. Phys. 82 (6) (2008)685-693 .
[24]. Navaneet Gupta, R C Gupta, Principles Of Materials Science And Engineering, Dhanapat Rai & Co. Pvt. Ltd. (2001) 79
[25]. Mahaligam T, Thanikarasan S And Chandramohon R, Mater. Sci Eng B, 174(2010)236
[26]. M Rasmani Devi And K Kunjabali Singh, International Journal Of Engineering And Technical Research (JETR) Vol. 9, Issue 12, Dec., (2019) 1-4
[27]. K Manikandan, P Mani, Fermi Hilbert Janbaraj, T Dominie Joshef, V Thangaraj, C Samendra Dilip And J Josheph Price, Indian Journal Of Pure & Applied Physics, Vol. 52, May (2014) 354-359
[28]. H P Klug And L E Alexander, X-Ray Diffraction Procedures, New York, John Willey & Sons Inc., (1954) 490
[29]. K. Kunjabali Singh And H. L. Das, Microstructures, Stress, Strain And Surface Characterization Of TD Polycrystalline Cds Thin Films, Indian J. Phys. 82 (6) (2008) 685-693.
[30]. M Rajesh Singh, K Zeetibala, M Malemnganbi And K Kunjabali Singh, IOSR Journal Of Electronics And Communication Engineering (IOSR-JECE) Vol. 21, Issue 1 (Jan-Feb ,2026) 06-11